Published in final edited form as:
Mol Cell Neurosci. 2008 February ; 37(2): 376–387.

Membrane depolarization inhibits spiral ganglion neurite growth via activation of multiple types of voltage sensitive calcium channels and calpain

Pamela C. Roehm[1,3], **Ningyong Xu**[1], **Erika A. Woodson**[1], **Steven H. Green**[1,2], and **Marlan R. Hansen**[1]

1 *Departments of Otolaryngology-Head and Neck Surgery, University of Iowa, Iowa City, Iowa 52242*

2 *Department of Biology, University of Iowa, Iowa City, Iowa 52242*

Abstract

The effect of membrane electrical activity on spiral ganglion neuron (SGN) neurite growth remains unknown despite its relevance to cochlear implant technology. We demonstrate that membrane depolarization delays the initial formation and inhibits the subsequent extension of cultured SGN neurites. This inhibition depends directly on the level of depolarization with higher levels of depolarization causing retraction of existing neurites. Cultured SGNs express subunits for L-type, N-type, and P/Q type voltage-gated calcium channels (VGCCs) and removal of extracellular Ca^{2+} or treatment with a combination of L-type, N-type, P/Q-type VGCC antagonists rescues SGN neurite growth under depolarizing conditions. By measuring the fluorescence intensity of SGNs loaded with the fluorogenic calpain substrate *t*-butoxy carbonyl-Leu-Met-chloromethylaminocoumarin (20 μM), we demonstrate that depolarization activates calpains. Calpeptin (15 μM), a calpain inhibitor, prevents calpain activation by depolarization and rescues neurite growth in depolarized SGNs suggesting that calpain activation contributes to the inhibition of neurite growth by depolarization.

Keywords

auditory neuron; axon growth; Ca^{2+}/calmodulin dependent kinase II

I. INTRODUCTION

Spiral ganglion neurons (SGNs) are bipolar neurons that transmit auditory information from the ear to the brain. The distal axon of the SGN synapses with inner ear hair cells while the proximal axon projects to the cochlear nucleus. SGNs critically depend on intact hair cells for continued survival. Following hair cell loss, SGN peripheral processes initially degenerate followed by a gradual loss of the SGNs themselves through apoptosis (Lee et al., 2003, Scarpidis et al., 2003, Ladrech et al., 2004, Alam et al., 2007). Multiple factors that increase SGN survival have been identified, including peptide neurotrophic factors such as neurotrophin-3 (NT-3) and brain derived neurotrophic factors (BDNF) (Staecker et al., 1996, Fritzsch et al., 1997, Miller et al., 1997, Mou et al., 1997, Roehm and Hansen, 2005). Membrane

Correspondence: Marlan R. Hansen, MD, Department of Otolaryngology-Head and Neck Surgery, 2PFP, University of Iowa Hospitals and Clinics, Iowa City, Iowa, 52242, Phone: (319) 353-7151, Fax: (319) 356-4547, Email: marlan-hansen@uiowa.edu.
[3]Current address: Department of Otolaryngology-Head and Neck Surgery, New York University, New York, NY 10016

electrical activity also provides a strong survival stimulus both *in vitro* and *in vivo.* Depolarization, accomplished by raising extracellular K^+ ($[K^+]_o$), promotes SGN survival *in vitro*(Hegarty et al., 1997) while direct electrical stimulation via an implanted electrode may increase SGN survival after hair cell loss (Lousteau, 1987, Hartshorn et al., 1991, Leake et al., 1991, Mitchell et al., 1997, Leake et al., 1999, Shepherd et al., 2005). Survival responses due to membrane electrical activity require Ca^{2+} influx through L-type voltage-gated calcium channels (VGCCs) (Hegarty et al., 1997, Mitchell et al., 1997) and subsequent activation of at least three separate calcium dependent protein kinases: cyclic AMP-dependent protein kinase (protein kinase A, PKA), and Ca^{2+}/calmodulin-dependent kinases II and IV (CaMKII, CaMKIV) (Hansen et al., 2001, Bok et al., 2003, Bok et al., 2007). However, excessive Ca^{2+} influx is toxic and leads to SGN death (Hegarty et al., 1997).

These Ca^{2+}-dependent signaling pathways regulate many aspects of neuronal function aside from survival, including neurite growth and guidance, synaptic maintenance and plasticity (Ghosh and Greenberg, 1995, Gomez and Spitzer, 2000, Zucker and Regehr, 2002, Collin et al., 2005). The effects of membrane electrical activity and $[Ca^{2+}]_i$ on SGN neurite growth have not been extensively investigated but it is clear that at least one Ca^{2+}-dependent signal, CaMKII, is a strong negative regulator of neurite growth (Hansen et al., 2003). Given the relevance of SGN axon regrowth to cochlear implant technology as well as the potential of hair cell regeneration (Izumikawa et al., 2005), we have explored the effects of membrane depolarization on SGN neurite extension *in vitro*. Increasing levels of $[K^+]_o$ leads to a dose-dependent decrease in SGN neurite lengths, even at levels which promote SGN survival. These effects on neurite outgrowth result from delayed formation of neurite processes as well as decreased extension of existing processes. This inhibition of neurite growth by depolarization involves multiple types voltage gated calcium channels and activation of calpain, a calcium-dependent protease.

II. METHODS

Spiral ganglion cultures

Dissociated spiral ganglion cultures were prepared as previously described (Hegarty et al., 1997, Hansen et al., 2001, Bok et al., 2003). Briefly, ganglia were dissected from postnatal day 5 (P5) rat pups, dissociated with trypsin, plated on polyornithine/laminin-coated 8-well culture chambers (Nalge Nunc International; Naperville, IL), and maintained in high glucose Dulbecco's Modified Eagle's Medium (DMEM) with N2 supplement (Invitrogen; Carlsbad, CA) and fresh insulin (10 μg/ml, Sigma-Aldrich; St. Louis, MO) in a humidified incubator with 6.5% CO_2. Three hr after plating the cultures were placed in experimental or control conditions, maintained for 48 hr to allow for neurite growth, and then fixed for immunofluorescence. We typically obtained ~1,000 SGNs/well in cultures maintained in NT3 (50 ng/ml) corresponding to ~2,000 SGNs/cochlea, similar to the plating efficiency of other methods of culturing rat SGNs (Ripoll and Rebillard, 1997).

Cultures were depolarized with elevated extracellular K^+ – 30 mM (30K) or 80 mM (80K) – or maintained in control nondepolarizing 5 mM K^+ (5K) medium, as previously described (Hegarty et al., 1997). Some cultures were depolarized in the presence of the following VGCC inhibitors singly or in combination: the L-type channel blocker verapamil (VPL, 10μM; Sigma), the N-type channel blocker ω–conotoxin GVIA (CTX, 1 μM; Calbiochem, San Diego, CA), and the P/Q-type channel blocker agatoxin (AGA, 1 μM; Calbiochem, San Diego, CA).

Gene transfer into SGNs

A different culture procedure was used for gene transfer into SGNs. Cultures were initially plated in serum-free medium containing NT-3 (50 ng/ml: RND systems; Minneapolis, MN) to

support SGN survival during transfection. Six to eight hours after plating (to allow time for attachment) the cultures were transfected with green fluorescent protein (GFP) -tagged autocamtide-2-related inhibitory peptide (GFP-AIP) or GFP-tagged control (scrambled) peptide (GFP-CON) (Bok et al., 2007) expression plasmids using calcium-phosphate precipitation as previously described (Zha et al., 2001, Hansen et al., 2003). Typically, this resulted in the transfection of 10–15% of the SGNs yielding approximately 130 transfected SGNs per well (Hansen et al., 2007). Twelve hours after transfection the medium was removed and replaced with NT-3-containing culture medium (depolarizing or control nondepolarizing) for an additional 48 hr.

For lentivirus-mediated gene transfer, cultures were maintained in serum-free NT-3-containing culture medium for 48 hr after plating to allow for neurite development. GFP-expressing feline immunodeficiency virus (GFP-FIV) stocks (typically $\approx 5\times10^7$ transforming units/ml) were obtained from the University of Iowa Gene Transfer Vector and added at a dilution of 1:100 to the culture medium in each well. The cultures were then depolarized with 30K for 3 hr to facilitate expression of the transgenes and maintained subsequently for an additional 24 hr in NT-3-containing medium. Expression of the GFP was evident within 24 hr after infection. Typically, this resulted in transfection of 70% of the SGNs. After viewing to record the locations of GFP-expressing SGNs, the cultures were maintained in NT-3 with either 5K, 30K or 80K for an additional 24 hr and then fixed and labeled with anti-NF-200 antibody.

Immunocytochemistry

Cultures were fixed with 4% paraformaldehyde for 10 minutes, permeabilized with 0.8% Triton-X in phosphate buffered saline (PBS) without Ca^{2+} and Mg^{2+} for 15 minutes. After a 20 minute incubation in “blocking buffer” (5% normal goat serum, 2% bovine serum albumin (BSA, Sigma-Aldrich, St. Louis, MO) and 0.1% Triton-X in PBS) to reduce nonspecific immunoreactivity, the cultures were immunolabeled with anti-neurofilament 200 (NF200) monoclonal antibody N52 (1:1000, Sigma-Aldrich, St. Louis, MO) that recognizes phosphorylated and unphosphorylated NF200 followed by an Alexa 568-labeled secondary antibody (1:800; Invitrogen, Carlsbad, CA) to visualize SGN somata and neurites.

Measurement of neurite length

Digital images of 5–7 random 10X fields per each experimental condition were captured on a Leica DMRIII microscope equipped with epifluorescence filters and a cooled CCD camera using Leica FW4000 software. Random fields were chosen by viewing cell nuclei to select fields with roughly comparable cell density. The investigator then captured images of the anti-NF200 immunofluorescence on the digital camera without prior viewing of the NF200 staining to eliminate bias towards selecting fields with different numbers of SGNs or neurite lengths. Neurite length was determined for each SGN within the field using the measurement tool in Image J (NIH; Bethesda, MD). For each condition, SGN neurites were measured from at least 3 separate cultures prepared at different times from different litters. Length is defined as the maximal possible distance along a neurite, i.e., the distance from the soma to the end of the longest neurite (if more than one neurite was present) and to the end of the longest branch at each branchpoint for branched neurites. If the longest neurite/branch of the chosen cell extended beyond the image border, additional images were acquired to include and measure the entire length of the process. Measurement of neurites in transfected SGNs was as above except that only GFP-expressing SGNs were scored as previously described (Hansen et al., 2007).

Calpain activity measurements

Dissociated spiral ganglion cultures were initially maintained in NT-3- and BDNF-supplemented medium (both 50 ng/ml). After 48 h, the cells were loaded with the cell-

permeable fluorogenic calpain substrate *t*-butoxy carbonyl-Leu-Met-chloromethylaminocoumarin (*t*-Boc-LM-CMAC) (20 μM; Molecular Probes; Eugene, OR) in DMEM/N2 media by incubation for 20 min followed by washing with DMEM. Cultures were then depolarized with 30K or 80K DMEM/N2 medium. Control cultures were treated with DMEM/N2 medium without elevated $[K^+]_o$. Some cultures were additionally treated with the calpain inhibitor calpeptin (Calp, Calbiochem); this was added to a final concentration of 15 μM 15 min prior to depolarization and remained in the culture during the depolarization. *t*-Boc-LM-CMAC fluorescence was imaged using a dichroic filter (excitation peak 350±25 nm, emission peak 460±25 nm, Chroma Technology Corp., Rockingham, VT). Fluorescence intensity was quantified using ImageJ software. A circle was drawn just inside the boundary of each neuronal soma and the average pixel density within the circle was measured. Background fluorescence was determined as the average pixel density within a circle of equal diameter just outside of the neuron boundary, and this background was subtracted from the value obtained for neuronal fluorescence. The scale used was arbitrary but consistent. We assayed at least 15 randomly selected neurons per condition in each of three repetitions using different cultures.

Statistical Analysis and Image Processing

Graphs were prepared using Excel software (Microsoft, Seattle, WA). Statistical analysis was done using SigmaStat (Systat Software, Inc; San Jose, CA). Significance of differences among treatment groups in neurite length measurements was determined by Kruskal-Wallis ANOVA on ranks followed by a post hoc Dunn's method. Significance of differences among treatment groups in measurements of the fraction of SGNs bearing a neurite was determined by ANOVA followed by post-hoc Holm-Sidak method using SigmaStat. Images were prepared for publication using Adobe Photoshop and Illustrator (Adobe Systems; San Jose, CA).

III. RESULTS

Membrane depolarization inhibits SGN neurite initiation

Dissociated cell cultures, prepared from P5 rat spiral ganglia, were maintained in NT-3 (50 ng/ml), a neurotrophic factor that promotes SGN survival and neurite growth (Lefebvre et al., 1991, Hegarty et al., 1997, Wittig et al., 2005), and depolarized with 30 mM $[K^+]_o$ (30K) or 80 mM $[K^+]_o$ (80K) and compared with nondepolarized SGNs in control (5K) medium. By using NT-3 to maintain SGN survival, we could dissociate effects of depolarization on survival from effects on neurites. After 48 hr, the cultures were fixed and immunolabeled with an anti-neurofilament 200 (NF-200) antibody that recognizes both phosphorylated and unphosphorylated neurofilament 200, followed by an Alexa 568 secondary antibody to allow visualization of the SGN somata and neurites by immunofluorescence. Five to seven randomly-chosen areas in each well were digitally imaged. Using ImageJ, neurite length was determined by measuring the longest process arising from each NF-200 positive SGN.

Figure 1 presents cumulative percent histograms of SGN neurite length. In these histograms conditions with shorter neurites are shifted to the left compared with conditions with longer neurites. Depolarization with 30K and 80K results in a dose-dependent decrease in SGN neurite length. This inhibition in neurite growth occurred in the presence of NT-3 and was statistically different for both NT-3+30K and NT-3+80K compared with NT-3 and with each other ($p<0.05$).

The inhibition of neurite growth by depolarization could result from delayed formation of a neurite process and/or by a reduction in the rate of neurite extension. To distinguish among these possibilities we first determined the rate of neurite formation in cultures maintained in NT-3, NT-3+30K, or NT-3+80K for 6, 12, 18, 24 and 48 hr after plating. SGNs were scored

as having no discernable neurite, a minor neurite (<1 cell diameter in length), or a major neurite (≥ 1 cell diameter in length). At least 100 SGNs were scored for each condition and the experiment was repeated three times with different cultures. The percentage of SGNs in each category was then determined and the data presented represent the average of the 3 repetitions. Figure 2 presents the average percent of SGNs bearing a minor or major neurite for each time point. At 6 hr, less than 5% of the SGNs had discernable neurites, and there was no statistically significant difference in the percent of SGNs bearing a neurite among the treatment conditions. At 12 hr, a significantly higher percentage of SGNs in NT-3 had a neurite compared with those in NT-3+30K ($p<0.001$, ANOVA followed by post-hoc Holm-Sidak method) and those in NT-3+80K ($p<0.001$). Similarly, at 12 hr a significantly higher percentage of SGNs in NT-3 +30K had a neurite compared with those in NT-3+80K ($p<0.001$). These differences persisted until the 48 hr time point at which point there was no longer a statistically significant difference between the percent of SGNs bearing a neurite in NT-3 compared with those in NT-3+30K ($p=0.057$). These results imply that depolarization delays the formation of neurites in SGNs.

Membrane depolarization inhibits SGN neurite extension and causes existing neurites to retract

To determine whether depolarization also inhibits SGN neurite extension we performed imaging of live SGNs with growing neurites. To observe SGNs and their neurites, we expressed green fluorescent protein (GFP) in the SGNs. This completely fills the somata and neurites allowing clear visualization of SGN morphology in live or fixed cells (Fig. 3) (Hansen et al., 2003,Hansen et al., 2007). To do so, we infected spiral ganglion cultures with a lentiviral (feline immunodeficiency virus, FIV) vector expressing GFP (FIV-GFP). Use of FIV-GFP effectively solves two problems. First, calcium phosphate-mediated transfection, which is an efficient means of gene transfer into freshly-plated SGNs, is less so for SGNs in established cultures that have already extended neurites. Second, the majority of the cells in our cultures are Schwann cells but FIV is highly selective to neurons. FIV, at the titer we use, infects approximately 70% of cultured SGNs but only a small percentage of non-neuronal cells (Fig. 3).

Cultures were initially maintained in NT-3 to promote survival and neurite growth. Forty-eight hours later, once neurites had formed, FIV-GFP was added to the cultures. Within 24 hr, GFP-expressing SGNs were evident, all of which had long neurites. At this time, 3 days *in vitro* (3 DIV), digital images were made of randomly chosen neurons and the positions of these neurons recorded. The cultures were then maintained in NT-3 and not depolarized (5K), in NT-3+30K, or in NT-3+80K. The cultures were fixed after a further 24 hr of culture and labeled for NF-200 immunofluorescence. Using the coordinates recorded at the first imaging, each SGN was imaged again, using both GFP fluorescence and NF-200 immunofluorescence (Fig. 3). All of the initially imaged neurons remained viable during the 24 hr period. Neurite lengths were measured as described in Methods. There was no difference in neurite lengths, whether GFP fluorescence or NF-200 immunofluorescence was used for measurement. The difference between the initial length (3 DIV) and final length (4 DIV) was then calculated for each SGN. These data are plotted in Fig. 3 as cumulative percent histograms with the data binned in 100 μm increments. Negative values represent neurite retraction while positive values represent neurite extension. Over 95% of SGNs in NT-3 without depolarization (control cultures) exhibited neurite extension. The rate of neurite extension was significantly reduced in depolarized cultures in 30K relative to control cultures ($p<0.05$). Depolarization with 80K (+NT-3) resulted in neurite retraction in 62% of the SGNs and significantly reduced extension for the remainder. Neurite growth in 80K was significantly ($p<0.05$) different from that in 30K or 5K (control) cultures.

These results demonstrate that depolarization delays SGN neurite formation and decreases extension of previously-formed neurites. Increasing depolarization results in increased inhibition of neurite growth and retraction of existing neurites. We next asked whether this involves Ca^{2+} entry via voltage-gated Ca^{2+} channels (VGCCs).

Extracellular Ca^{2+} is required for inhibition of neurite growth by depolarization

Growth cone dynamics, including responsiveness to extracellular cues, turning, and extension, critically depend on intracellular calcium concentration; in particular, excessive $[Ca^{2+}]_i$ inhibits neurite extension (Gomez and Zheng, 2006). We hypothesized that the ability of depolarization to inhibit SGN neurite growth depends on Ca^{2+} influx, presumably via VGCCs. To determine whether extracellular Ca^{2+} is required for inhibition of neurite growth by depolarization, we cultured SGNs in medium lacking Ca^{2+} but containing the Ca^{2+} chelator EGTA. The cultures were then depolarized with 30K or 80K in the presence of NT-3 (50 ng/ml). Relative to cultures in maintained in standard medium ($[Ca^{2+}]_o$ = 1.8 mM), cultures lacking extracellular Ca^{2+} showed significantly ($p<0.05$) increased neurite growth in 30K and in 80K (Fig. 4). Removal of extracellular Ca^{2+}, which can lower intracellular Ca^{2+} levels, had no significant effect on neurite growth in NT-3 without depolarization. These observations suggest that the inhibition of neurite growth by depolarization depends on entry of extracellular Ca^{2+}, presumably via VGCCs.

Multiple types of VGCCs contribute to the inhibition of neurite growth by depolarization

We immunolabeled spiral ganglion cultures maintained in NT-3 for 24 hr with antibodies against L, N, and P/Q type VGCCs, colabeling with anti-NF-200 to visualize SGN cell bodies and neurites. As shown in Fig. 5, cultured SGNs express subunits for α1C (L-type), α1B (N-type), and α1A (P/Q-type) VGCC subunits. Consistent with previous reports (Trimmer and Rhodes, 2004), α1C subunits were enriched in the cell body while α1B and α1A were more evenly distributed throughout the entire SGN, including the neurites. Thus, cultured rat SGNs express multiple types of VGCCs, with N-type and P/Q-type being ubiquitous and L-type preferentially somatic.

We next asked whether these VGCCs are indeed involved in inhibition of neurite growth by depolarization and, if so, which type(s). Treatment with the L-type channel blocker verapamil (VPL, 10 μM) resulted in a statistically significant ($p<0.05$, Kruskal-Wallis ANOVA on Ranks, Dunn's post-hoc comparison) increase in neurite length for cultures in either NT3+30K or NT3 +80K. These neurites, however, were still significantly shorter than those in NT3 without depolarization ($p<0.05$), implying that VGCCs other than L-type also contribute to inhibition of neurite growth by depolarization. To test this possibility, we treated spiral ganglion cultures with ω-conotoxin GVIA (CTX, 1 μM), an N-type VGCC antagonist, or with agatoxin (AGA, 1 μM), a P/Q VGCC antagonist. Inhibition of SGN neurite growth by depolarization in 30K or in 80K was partially rescued by CTX or by AGA (Fig. 6) and combining VPL, CTX, and AGA provided a rescue significantly ($p<0.05$) greater than any of the VGCC antagonists used singly (Fig. 6). Thus, inhibition of neurite growth by depolarization requires Ca^{2+} entry through multiple types of VGCCs. This contrasts with the prosurvival effects of depolarization, which are completely abolished by L-type VGCC antagonists and unaffected by CTX (Hegarty et al., 1997). This may reflect a particular requirement in prosurvival signaling for Ca^{2+} entry into the soma, where L-type channels are enriched.

CaMKII is not necessary for inhibition of SGN neurite growth by depolarization

There are many Ca^{2+}-regulated proteins that could mediate the observed effects on neurite growth. CaMKII, CaMKIV, and PKA are Ca^{2+}-activated and are recruited by depolarization to promote SGN survival (Hansen et al., 2001, Bok et al., 2003, Hansen et al., 2003). Overexpression of a C-terminal-truncated CaMKII (CaMKII(1–290)) that is constitutively

active, while promoting SGN survival, strongly inhibits SGN neurite growth (Hansen et al., 2003). Therefore, we sought to determine the extent to which CaMKII activation is necessary for the inhibitory effects of depolarization on SGN neurites. To inhibit CaMKII activity, we transfected SGNs with a chimeric protein consisting of green fluorescent protein fused to the autocamtide-2-related inhibitory peptide (GFP-AIP) (Bok et al., 2007). The AIP moiety binds specifically to the catalytic site of CaMKII to inhibit the kinase activity (Ishida et al., 1995). GFP-AIP effectively and specifically inhibits CaMKII activity and inhibits survival in elevated $[K^+]_o$ when expressed in SGNs (Bok et al., 2007). SGN cultures were transfected with GFP-AIP and then maintained in NT-3, NT-3+30K, or NT-3+80K for 48 hr. Control cultures were transfected with GFP-CON, in which AIP is replaced with a control (scrambled) peptide that does not inhibit CaMKII. SGN neurite length was determined as above for transfected SGNs, scoring only GFP and NF-200 positive cells. Overexpression of GFP-AIP failed to rescue SGN neurites from growth inhibition by either 30K or 80K (Fig. 7).

To confirm that CaMK activity does not contribute to the inhibitory effects of depolarization, we treated SGN cultures with KN-62 (10 μM), a CaMK inhibitor that reduces SGN survival in response to depolarization (Tokumitsu et al., 1990, Hansen et al., 2003). Like GFP-AIP, KN-62 failed to prevent the inhibition of SGN neurite growth by depolarization. Thus, CaMKII activity inhibits SGN neurite growth and is required for the prosurvival effect of depolarization, but it is not independently necessary for the inhibition of SGN neurite growth by depolarization. These data imply that, although a high level of CaMKII activity is sufficient to inhibit neurite growth (Hansen et al., 2003), depolarization, presumably, activates Ca^{2+}-dependent signals other than CaMKII that also contribute to inhibition of neurite growth so inhibition only of CaMKII has no significant effect.

Calpain activity is necessary for the inhibition of neurite growth by depolarization

Calpains are Ca^{2+}-sensitive proteases implicated in negative regulation of growth cone behavior by Ca^{2+} (Robles et al., 2003). We tested the possibility that calpains are activated by depolarization in SGNs and that calpain activity is necessary for the inhibition of SGN neurite growth by depolarization. We first quantified calpain activity in depolarized SGNs using cell-permeable fluorogenic calpain substrate *t*-butoxy carbonyl-Leu-Met-chloromethylaminocoumarin (Boc-LM-CMAC) (Rosser et al., 1993, Glading et al., 2000). After loading with Boc-LM-CMAC, the spiral ganglion cultures were treated with 30K or 80K in the presence or absence of the calpain inhibitor calpeptin (15 μM) for 15 minutes. Control cultures were maintained in 5.4 mM $[K^+]_o$. Images of Boc-LM-CMAC fluorescence were captured for 15–20 randomly selected SGNs for each condition. Boc-LM-CMAC fluorescence was quantified as the average pixel intensity in a region of interest (ROI) drawn just inside the SGN soma. To correct for background, the pixel intensity from a similarly sized ROI drawn just outside the soma was subtracted from the Boc-LM-CMAC fluorescence for each SGN. Representative images are in Fig. 8.

Depolarization with 30K and 80K resulted in a significant increase in Boc-LM-CMAC fluorescence compared with control cultures (Fig. 8) ($p<0.05$ by Kruskal-Wallis ANOVA on ranks followed by Dunn's post-hoc comparison). The increase in Boc-LM-CMAC fluorescence was blocked by calpeptin, confirming that calpeptin significantly ($p<0.05$) inhibits calpain activation by depolarization. Results of a representative experiment are presented in Fig. 8 (similar results were obtained in 2 separate repetitions).

Having confirmed that calpains are activated by depolarization, we next asked whether calpain activity is required for the inhibition of SGN neurite growth by depolarization. SGN cultures were maintained for 48 hr in NT-3, NT-3+30K, or NT-3+80K in the presence or absence of calpeptin (15 μM). Neurite lengths for each condition were determined as above and are presented as cumulative histograms in Fig. 9. SGN neurites in NT-3+30K+calpeptin and NT-3

+80K+calpeptin were significantly ($p<0.05$ by Kruskal-Wallis ANOVA on ranks followed by Dunn's post-hoc comparison) longer than neurites in NT-3+30K and NT-3+80K, respectively, but were not significantly different from neurites in NT-3 only. Thus, calpain activation contributes to the inhibition of neurite growth by depolarization.

IV. DISCUSSION

Membrane depolarization inhibits SGN neurite growth via Ca^{2+} entry through VGCCs

We have demonstrated that membrane electrical activity in the form of depolarization inhibits neurite growth in early postnatal rat SGNs. This inhibition is due to a reduction in the rate of extension of SGN neurites that have already formed, as well as a delay in the initial neurite formation. We have previously shown that steady state $[Ca^{2+}]_i$ increases with increasing depolarization and that moderately elevated $[Ca^{2+}]_i$ is optimal for SGN survival (Hegarty et al., 1997). Higher levels of depolarization, e.g. 80K, which reduce SGN survival (Hegarty et al., 1997), also cause retraction of existing neurites, even in the presence of the neurotrophin, NT-3. We have previously shown (Hegarty et al., 1997) that the toxic effect of strong depolarization is correlated with high $[Ca^{2+}]_i$. Removal of extracellular Ca^{2+} from the culture medium or blockade of VGCCs prevents the inhibition of neurite growth by depolarization, indicating that this is also due to elevated $[Ca^{2+}]_i$. These observations confirm a causal role of Ca^{2+} entry in the reduction of SGN neurite growth by membrane depolarization and are consistent with the ability of $[Ca^{2+}]_i$ dynamics to negatively regulate growth cone extension and neurite growth (Fields et al., 1990, Kater and Mills, 1991, Gu et al., 1994, Gomez et al., 1995, Arcaro and Lnenicka, 1997, Gomez and Spitzer, 1999, Ibarretxe et al., 2007, Iizuka et al., 2007). Changes in $[Ca^{2+}]_i$ can affect neurofilament expression (Bui et al., 2003). However, our findings were similar whether based on NF200 immunoreactivity or GFP fluorescence, which fills the soma and the entire neurite process. Also, we detected no difference in NF200 immunolabeling in the SGN somata among the various conditions further confirming that the differences in neurite lengths were not simply due to changes in neurofilament expression.

Despite the many studies linking changes in $[Ca^{2+}]_i$ to the regulation of neurite growth, the specific downstream effectors that transduce Ca^{2+} signals into corresponding growth cone behavior remain largely unknown. Depolarization activates several Ca^{2+}-regulated proteins that could potentially mediate the observed effects on SGN neurite growth. The kinases CaMKII, CaMKIV and PKA are recruited by depolarization to promote SGN survival (Hansen et al., 2001, Bok et al., 2003, Hansen et al., 2003, Bok et al., 2007). Depolarization activates CaMKII in SGNs and CaMKII activity inhibits SGN neurite growth (Hansen et al., 2003), making CaMKII a potential candidate to mediate the effects of depolarization on SGN neurite growth (Bolsover, 2005). However, we show here that CaMKII inhibitors (GFP-AIP and KN-62) fail to rescue neurite growth during depolarization indicating that CaMKII does not independently contribute to the effects of depolarization on neurite growth.

Activation of the Ca^{2+}-dependent phosphatase calcineurin (protein phosphatase 2B, PP2B), has been shown to regulate growth cone motility and axon regeneration (Lyons et al., 1994, Chang et al., 1995, Wen et al., 2004, Bolsover, 2005). In SGNs, calcineurin inhibitors – cyclosporin A and FK506 – fail to rescue neurite growth in depolarized SGNs (Supplemental Fig. 1), implying that calcineurin does not play an independent role in the inhibition of neurite growth by depolarization in SGNs.

Role of calpain activity on SGN neurite growth

In this study, we identify the Ca^{2+}-sensitive neutral protease, calpain, as an essential downstream effector of depolarization. Depolarization leads to calpain activation and inhibition of calpains rescues neurite growth in depolarized SGNs. These results are consistent

with observations in other neurons showing that calpains regulate growth cone formation, motility and guidance in response to Ca^{2+} signals (Oshima et al., 1989, Song et al., 1994, Shea et al., 1995, Gitler and Spira, 1998, Robles et al., 2003, Spira et al., 2003). Several molecules that regulate cell adhesion and motility are known calpain substrates including nonreceptor protein kinases (Carragher et al., 2003, Sawhney et al., 2006), phosphatases (Wu et al., 2004, Liu et al., 2005), cytoskeleton-associated proteins (Nixon, 1986, Yamaguchi et al., 1994, Dourdin et al., 2001, Franco et al., 2004), and adhesion molecules (β-integrins) (Huttenlocher et al., 1997, Xi et al., 2006). Additonally, calpains may influence growth cone behavior by modulating tyrosine kinase signaling within the growth cone (Robles et al., 2003).

Differences in the effects of depolarization on neurite outgrowth and neuron survival

The mechanisms leading to inhibition of neurite growth by depolarization differ from those recruited to promote SGN survival. First, the survival response to depolarization demonstrates a biphasic response to the level of depolarization—the best survival response is achieved in 25–30 mM $[K^+]_o$ while lower or higher levels of $[K^+]_o$ lead to diminished survival (Hegarty et al., 1997). In contrast, depolarization reduces neurite growth in a dose-dependent fashion. Second, L-type VGCC antagonists completely abolish the prosurvival effects of depolarization (Hegarty et al., 1997, Miller et al., 2003), but only partially rescue SGN neurite growth in depolarized cultures. Further, N-type VGCC antagonists do not reduce depolarization-mediated SGN survival (Hegarty et al., 1997). In contrast, N- and P/Q-type VGCCs contribute in an additive fashion with L-type VGCCs to the inhibition of neurite growth by depolarization. Third, as mentioned above, CaMKII activity is required for the prosurvival effects of depolarization (Hansen et al., 2001, Bok et al., 2007). Conversely, CaMKII is not independently required for the inhibition of neurite growth by depolarization even though overexpression of a constitutively active CaMKII mutant strongly inhibits SGN neurite growth (Hansen et al., 2003). These differences suggest that it may be possible to selectively prevent the reduction in neurite growth by depolarization without affecting the prosurvival response.

Implications for cochlear implant technology

SGNs are not only crucial for normal hearing but also convey sound information from cochlear implants (CIs) to the brain. Multichannel CIs placed in the cochlea restore functional auditory perception in deaf patients by directly stimulating the SGNs (Rubinstein, 2004), replacing the function of lost hair cells. Outcomes with current CIs are limited by current spread and channel interactions leading to significantly diminished spectral and temporal resolution (Rubinstein, 2004). Regrowth of SGN peripheral axons toward the stimulating electrodes might allow reduced currents, more refined stimulation paradigms, and improved functional outcomes (Rubinstein, 2004). Thus, there is growing interest in therapeutic strategies to induce regrowth of SGN peripheral processes towards a stimulating electrode (Bianchi and Raz, 2004, Roehm and Hansen, 2005, Wittig et al., 2005, Evans et al., 2007). To the extent that chronic depolarization mimics electrical stimulation *in vivo* (Hegarty et al., 1997, Miller et al., 2003), inhibition of neurite outgrowth by depolarization suggests an additional consideration in the development of such strategies.

Chronic depolarization, as used in these studies, however may not accurately mimic electrical stimulation provided by a cochlear implant, which consists of pulses of brief depolarization. For example, the route of Ca^{2+} entry differs depending on whether cultured sensory neurons are chronically depolarized or electrically stimulated in a pulsatile pattern, being predominantly through L-type VGCCs in the former case but also through N-type in the latter (Hegarty et al., 1997, Brosenitsch and Katz, 2001, Zhao et al., 2007). Of note, in SGNs, L-type calcium channels are required for survival signaling by chronic depolarization *in vitro* and by electrical stimulation via an implanted electrode *in vivo* (Han et al., 1994, Hegarty et al., 1997, Miller et al., 2003). Further, our studies used SGNs cultured from early postnatal, rather than adult, rats.

The response of these neurons to chronic or pulsatile depolarization may differ from the response of adult neurons.

In conclusion, we find that chronic membrane depolarization inhibits SGN neurite growth and that this effect is mediated by Ca^{2+} influx via L-, N-, and P/Q VGCCs and activation of calpain. This contrasts to the mechanisms recruited by depolarization to promote SGN survival, which are mediated by CaMKII, CaMKII, and PKA activation. By selectively targeting calpains, it may be possible to prevent the inhibition of neurite growth by membrane electrical activity while preserving the prosurvival effects. Such strategies could potentially benefit patients receiving cochlear implants, allowing optimal SGN neurite outgrowth without disrupting the survival advantages of electrical stimulation.

Supplementary Material

Refer to Web version on PubMed Central for supplementary material.

Acknowledgements

Support for this study was provided by the American Otological Society (MRH), the American Hearing Research Foundation (SHG), NIDCD KO8 DC006211 (MRH), and NIDCD R01 DC02961 (SHG). The authors wish to thank associates of the Gene Transfer Vector Core Facility of the University of Iowa Center for Gene Therapy of Cystic Fibrosis and Other Genetic Diseases, supported by NIH/NIDDK P30 DK 54759 for their assistance with viral vector production.

References

Alam SA, Robinson BK, Huang J, Green SH. Prosurvival and proapoptotic intracellular signaling in rat spiral ganglion neurons in vivo after the loss of hair cells. J Comp Neurol 2007;503:832–852. [PubMed: 17570507]

Arcaro KF, Lnenicka GA. Differential effects of depolarization on the growth of crayfish tonic and phasic motor axons in culture. J Neurobiol 1997;33:85–97. [PubMed: 9212072]

Bianchi LM, Raz Y. Methods for providing therapeutic agents to treat damaged spiral ganglion neurons. Curr Drug Targets CNS Neurol Disord 2004;3:195–199. [PubMed: 15180480]

Bok J, Huang J, Wang Q, Green SH. CaMKII and CaMKIV mediate divergent prosurvival signaling pathways in response to depolarization in neurons. Mol Cell Neurosci. 2007in press

Bok J, Zha XM, Cho YS, Green SH. An extranuclear locus of cAMP-dependent protein kinase action is necessary and sufficient for promotion of spiral ganglion neuronal survival by cAMP. J Neurosci 2003;23:777–787. [PubMed: 12574406]

Bolsover SR. Calcium signalling in growth cone migration. Cell Calcium 2005;37:395–402. [PubMed: 15820386]

Brosenitsch TA, Katz DM. Physiological patterns of electrical stimulation can induce neuronal gene expression by activating N-type calcium channels. J Neurosci 2001;21:2571–2579. [PubMed: 11306610]

Bui CJ, Beaman-Hall CM, Vallano ML. Ca2+ and CaM kinase regulate neurofilament expression. Neuroreport 2003;14:2073–2077. [PubMed: 14600500]

Carragher NO, Westhoff MA, Fincham VJ, Schaller MD, Frame MC. A novel role for FAK as a protease-targeting adaptor protein: regulation by p42 ERK and Src. Curr Biol 2003;13:1442–1450. [PubMed: 12932330]

Chang HY, Takei K, Sydor AM, Born T, Rusnak F, Jay DG. Asymmetric retraction of growth cone filopodia following focal inactivation of calcineurin. Nature 1995;376:686–690. [PubMed: 7544441]

Collin T, Marty A, Llano I. Presynaptic calcium stores and synaptic transmission. Curr Opin Neurobiol 2005;15:275–281. [PubMed: 15919193]

Dourdin N, Bhatt AK, Dutt P, Greer PA, Arthur JS, Elce JS, Huttenlocher A. Reduced cell migration and disruption of the actin cytoskeleton in calpain-deficient embryonic fibroblasts. J Biol Chem 2001;276:48382–48388. [PubMed: 11602605]

Evans AR, Euteneuer S, Chavez E, Mullen LM, Hui EE, Bhatia SN, Ryan AF. Laminin and fibronectin modulate inner ear spiral ganglion neurite outgrowth in an in vitro alternate choice assay. Dev Neurobiol. 2007

Fields RD, Neale EA, Nelson PG. Effects of patterned electrical activity on neurite outgrowth from mouse sensory neurons. J Neurosci 1990;10:2950–2964. [PubMed: 2398369]

Franco SJ, Rodgers MA, Perrin BJ, Han J, Bennin DA, Critchley DR, Huttenlocher A. Calpain-mediated proteolysis of talin regulates adhesion dynamics. Nat Cell Biol 2004;6:977–983. [PubMed: 15448700]

Fritzsch B, Silos-Santiago I, Bianchi LM, Fariñas I. The role of neurotrophic factors in regulating the development of inner ear innervation. Trends Neurosci 1997;20:159–164. [PubMed: 9106356]

Ghosh A, Greenberg ME. Calcium signaling in neurons: molecular mechanisms and cellular consequences. Science 1995;268:239–247. [PubMed: 7716515]

Gitler D, Spira ME. Real time imaging of calcium-induced localized proteolytic activity after axotomy and its relation to growth cone formation. Neuron 1998;20:1123–1135. [PubMed: 9655501]

Glading A, Chang P, Lauffenburger DA, Wells A. Epidermal growth factor receptor activation of calpain is required for fibroblast motility and occurs via an ERK/MAP kinase signaling pathway. J Biol Chem 2000;275:2390–2398. [PubMed: 10644690]

Gomez TM, Snow DM, Letourneau PC. Characterization of spontaneous calcium transients in nerve growth cones and their effect on growth cone migration. Neuron 1995;14:1233–1246. [PubMed: 7605634]

Gomez TM, Spitzer NC. In vivo regulation of axon extension and pathfinding by growth-cone calcium transients. Nature 1999;397:350–355. [PubMed: 9950427]

Gomez TM, Spitzer NC. Regulation of growth cone behavior by calcium: new dynamics to earlier perspectives. J Neurobiol 2000;44:174–183. [PubMed: 10934320]

Gomez TM, Zheng JQ. The molecular basis for calcium-dependent axon pathfinding. Nat Rev Neurosci 2006;7:115–125. [PubMed: 16429121]

Gu X, Olson EC, Spitzer NC. Spontaneous neuronal calcium spikes and waves during early differentiation. J Neurosci 1994;14:6325–6335. [PubMed: 7965039]

Han D-Y, Harada N, Tomoda K, Yamashita T. Characterization of the calcium influx induced by depolarization of guinea pig cochlear spiral ganglion cells. ORL 1994;56:125–129. [PubMed: 7515485]

Hansen MR, Bok J, Devaiah AK, Zha XM, Green SH. Ca2+/calmodulin-dependent protein kinases II and IV both promote survival but differ in their effects on axon growth in spiral ganglion neurons. J Neurosci Res 2003;72:169–184. [PubMed: 12671991]

Hansen MR, Roehm PC, Xu N, Green SH. Overexpression of Bcl-2 or Bcl-xL prevents spiral ganglion neuron death and inhibits neurite growth. Dev Neurobiol 2007;67:316–325. [PubMed: 17443790]

Hansen MR, Zha XM, Bok J, Green SH. Multiple distinct signal pathways, including an autocrine neurotrophic mechanism, contribute to the survival-promoting effect of depolarization on spiral ganglion neurons in vitro. J Neurosci 2001;21:2256–2267. [PubMed: 11264301]

Hartshorn DO, Miller JM, Altschuler RA. Protective effect of electrical stimulation in the deafened guinea pig cochlea. Otolaryngology - Head & Neck Surgery 1991;104:311–319. [PubMed: 1902931]

Hegarty JL, Kay AR, Green SH. Trophic support of cultured spiral ganglion neurons by depolarization exceeds and is additive with that by neurotrophins or cyclic AMP, and requires elevation of $[Ca^{2+}]_i$ within a set range. J Neurosci 1997;17:1959–1970. [PubMed: 9045725]

Huttenlocher A, Palecek SP, Lu Q, Zhang W, Mellgren RL, Lauffenburger DA, Ginsberg MH, Horwitz AF. Regulation of cell migration by the calcium-dependent protease calpain. J Biol Chem 1997;272:32719–32722. [PubMed: 9407041]

Ibarretxe G, Perrais D, Jaskolski F, Vimeney A, Mulle C. Fast regulation of axonal growth cone motility by electrical activity. J Neurosci 2007;27:7684–7695. [PubMed: 17634363]

Iizuka A, Sengoku K, Iketani M, Nakamura F, Sato Y, Matsushita M, Nairn AC, Takamatsu K, Goshima Y, Takei K. Calcium-induced synergistic inhibition of a translational factor eEF2 in nerve growth cones. Biochem Biophys Res Commun 2007;353:244–250. [PubMed: 17187762]

Ishida A, Kameshita I, Okuno S, Kitani T, Fujisawa H. A novel highly specific and potent inhibitor of calmodulin-dependent protein kinase II. Biochem Biophys Res Commun 1995;212:806–812. [PubMed: 7626114]

Izumikawa M, Minoda R, Kawamoto K, Abrashkin KA, Swiderski DL, Dolan DF, Brough DE, Raphael Y. Auditory hair cell replacement and hearing improvement by Atoh1 gene therapy in deaf mammals. Nat Med 2005;11:271–276. [PubMed: 15711559]

Kater SB, Mills LR. Regulation of growth cone behavior by calcium. J Neurosci 1991;11:891–899. [PubMed: 2010811]

Ladrech S, Guitton M, Saido T, Lenoir M. Calpain activity in the amikacin-damaged rat cochlea. J Comp Neurol 2004;477:149–160. [PubMed: 15300786]

Leake PA, Hradek GT, Rebscher SJ, Snyder RL. Chronic intracochlear electrical stimulation induces selective survival of spiral ganglion neurons in neonatally deafened cats. Hearing Res 1991;54:251–271.

Leake PA, Hradek GT, Snyder RL. Chronic electrical stimulation by a cochlear implant promotes survival of spiral ganglion neurons after neonatal deafness. J Comp Neurol 1999;412:543–562. [PubMed: 10464355]

Lee JE, Nakagawa T, Kim TS, Iguchi F, Endo T, Dong Y, Yuki K, Naito Y, Lee SH, Ito J. A novel model for rapid induction of apoptosis in spiral ganglions of mice. Laryngoscope 2003;113:994–999. [PubMed: 12782811]

Lefebvre PP, Van de Water TR, Weber T, Rogister B, Moonen G. Growth factor interactions in cultures of dissociated adult acoustic ganglia: neuronotrophic effects. Brain Res 1991;567:306–312. [PubMed: 1817733]

Liu F, Grundke-Iqbal I, Iqbal K, Oda Y, Tomizawa K, Gong CX. Truncation and activation of calcineurin A by calpain I in Alzheimer disease brain. J Biol Chem 2005;280:37755–37762. [PubMed: 16150694]

Lousteau RJ. Increased spiral ganglion cell survival in electrically stimulated deafened guinea pig cochleae. Laryngoscope 1987;97:836–842. [PubMed: 3600136]

Lyons WE, George EB, Dawson TM, Steiner JP, Snyder SH. Immunosuppressant FK506 promotes neurite outgrowth in cultures of PC12 cells and sensory ganglia. Proc Natl Acad Sci U S A 1994;91:3191–3195. [PubMed: 7512727]

Miller AL, Prieskorn DM, Altschuler RA, Miller JM. Mechanism of electrical stimulation-induced neuroprotection: effects of verapamil on protection of primary auditory afferents. Brain Res 2003;966:218–230. [PubMed: 12618345]

Miller JM, Chi DH, O'Keeffe LJ, Kruszka P, Raphael Y, Altschuler RA. Neurotrophins can enhance spiral ganglion cell survival after inner hair cell loss. Int J Dev Neurosci 1997;15:631–643. [PubMed: 9263039]

Mitchell A, Miller JM, Finger PA, Heller JW, Raphael Y, Altschuler RA. Effects of chronic high-rate electrical stimulation on the cochlea and eighth nerve in the deafened guinea pig. Hear Res 1997;105:30–43. [PubMed: 9083802]

Mou K, Hunsberger CL, Cleary JM, Davis RL. Synergistic effects of BDNF and NT-3 on postnatal spiral ganglion neurons. J Comp Neurol 1997;386:529–539. [PubMed: 9378849]

Nixon RA. Fodrin degradation by calcium-activated neutral proteinase (CANP) in retinal ganglion cell neurons and optic glia: preferential localization of CANP activities in neurons. J Neurosci 1986;6:1264–1271. [PubMed: 3012012]

Oshima M, Koizumi S, Fujita K, Guroff G. Nerve growth factor-induced decrease in the calpain activity of PC12 cells. J Biol Chem 1989;264:20811–20816. [PubMed: 2555371]

Ripoll C, Rebillard G. A simple technique to efficiently dissociate primary auditory neurons from 5 day-old rat cochleas. J Neurosci Methods 1997;73:123–128. [PubMed: 9196282]

Robles E, Huttenlocher A, Gomez TM. Filopodial Calcium Transients Regulate Growth Cone Motility and Guidance through Local Activation of Calpain. Neuron 2003;38:597–609. [PubMed: 12765611]

Roehm PC, Hansen MR. Strategies to preserve or regenerate spiral ganglion neurons. Curr Opin Otolaryngol Head Neck Surg 2005;13:294–300. [PubMed: 16160524]

Rosser BG, Powers SP, Gores GJ. Calpain activity increases in hepatocytes following addition of ATP. Demonstration by a novel fluorescent approach. J Biol Chem 1993;268:23593–23600. [PubMed: 8226886]

Rubinstein JT. How cochlear implants encode speech. Curr Opin Otolaryngol Head Neck Surg 2004;12:444–448. [PubMed: 15377959]

Sawhney RS, Cookson MM, Omar Y, Hauser J, Brattain MG. Integrin alpha2-mediated ERK and calpain activation play a critical role in cell adhesion and motility via focal adhesion kinase signaling: identification of a novel signaling pathway. J Biol Chem 2006;281:8497–8510. [PubMed: 16461767]

Scarpidis U, Madnani D, Shoemaker C, Fletcher CH, Kojima K, Eshraghi AA, Staecker H, Lefebvre P, Malgrange B, Balkany TJ, Van De Water TR. Arrest of apoptosis in auditory neurons: implications for sensorineural preservation in cochlear implantation. Otol Neurotol 2003;24:409–417. [PubMed: 12806293]

Shea TB, Cressman CM, Spencer MJ, Beermann ML, Nixon RA. Enhancement of neurite outgrowth following calpain inhibition is mediated by protein kinase C. J Neurochem 1995;65:517–527. [PubMed: 7616205]

Shepherd RK, Coco A, Epp SB, Crook JM. Chronic depolarization enhances the trophic effects of brain-derived neurotrophic factor in rescuing auditory neurons following a sensorineural hearing loss. J Comp Neurol 2005;486:145–158. [PubMed: 15844207]

Song DK, Malmstrom T, Kater SB, Mykles DL. Calpain inhibitors block Ca(2+)-induced suppression of neurite outgrowth in isolated hippocampal pyramidal neurons. J Neurosci Res 1994;39:474–481. [PubMed: 7884824]

Spira ME, Oren R, Dormann A, Gitler D. Critical calpain-dependent ultrastructural alterations underlie the transformation of an axonal segment into a growth cone after axotomy of cultured Aplysia neurons. J Comp Neurol 2003;457:293–312. [PubMed: 12541311]

Staecker H, Kopke R, Malgrange B, Lefebvre P, Van de Water TR. NT-3 and/or BDNF therapy prevents loss of auditory neurons following loss of hair cells. Neuroreport 1996;7:889–894. [PubMed: 8724667]

Tokumitsu H, Chijiwa T, Hagiwara M, Mizutani A, Terasawa M, Hidaka H. KN-62, 1-[N,O-bis(5-isoquinolinesulfonyl)-N-methyl-L-tyrosyl]-4-phenylpiperazine, a specific inhibitor of Ca^{2+}/calmodulin-dependent protein kinase II. J Biol Chem 1990;265:4315–4320. [PubMed: 2155222]

Trimmer JS, Rhodes KJ. Localization of voltage-gated ion channels in mammalian brain. Annu Rev Physiol 2004;66:477–519. [PubMed: 14977411]

Wen Z, Guirland C, Ming GL, Zheng JQ. A CaMKII/calcineurin switch controls the direction of Ca(2+)-dependent growth cone guidance. Neuron 2004;43:835–846. [PubMed: 15363394]

Wittig JH Jr, Ryan AF, Asbeck PM. A reusable microfluidic plate with alternate-choice architecture for assessing growth preference in tissue culture. J Neurosci Methods 2005;144:79–89. [PubMed: 15848242]

Wu HY, Tomizawa K, Oda Y, Wei FY, Lu YF, Matsushita M, Li ST, Moriwaki A, Matsui H. Critical role of calpain-mediated cleavage of calcineurin in excitotoxic neurodegeneration. J Biol Chem 2004;279:4929–4940. [PubMed: 14627704]

Xi X, Flevaris P, Stojanovic A, Chishti A, Phillips DR, Lam SC, Du X. Tyrosine phosphorylation of the integrin beta 3 subunit regulates beta 3 cleavage by calpain. J Biol Chem 2006;281:29426–29430. [PubMed: 16935858]

Yamaguchi R, Maki M, Hatanaka M, Sabe H. Unphosphorylated and tyrosine-phosphorylated forms of a focal adhesion protein, paxillin, are substrates for calpain II in vitro: implications for the possible involvement of calpain II in mitosis-specific degradation of paxillin. FEBS Lett 1994;356:114–116. [PubMed: 7988702]

Zha XM, Bishop JF, Hansen MR, Victoria L, Abbas PJ, Mouradian MM, Green SH. BDNF synthesis in spiral ganglion neurons is constitutive and CREB- dependent. Hear Res 2001;156:53–68. [PubMed: 11377882]

Zhao R, Liu L, Rittenhouse AR. Ca2+ influx through both L- and N-type Ca2+ channels increases c-fos expression by electrical stimulation of sympathetic neurons. Eur J Neurosci 2007;25:1127–1135. [PubMed: 17331208]

Zucker RS, Regehr WG. Short-term synaptic plasticity. Annu Rev Physiol 2002;64:355–405. [PubMed: 11826273]

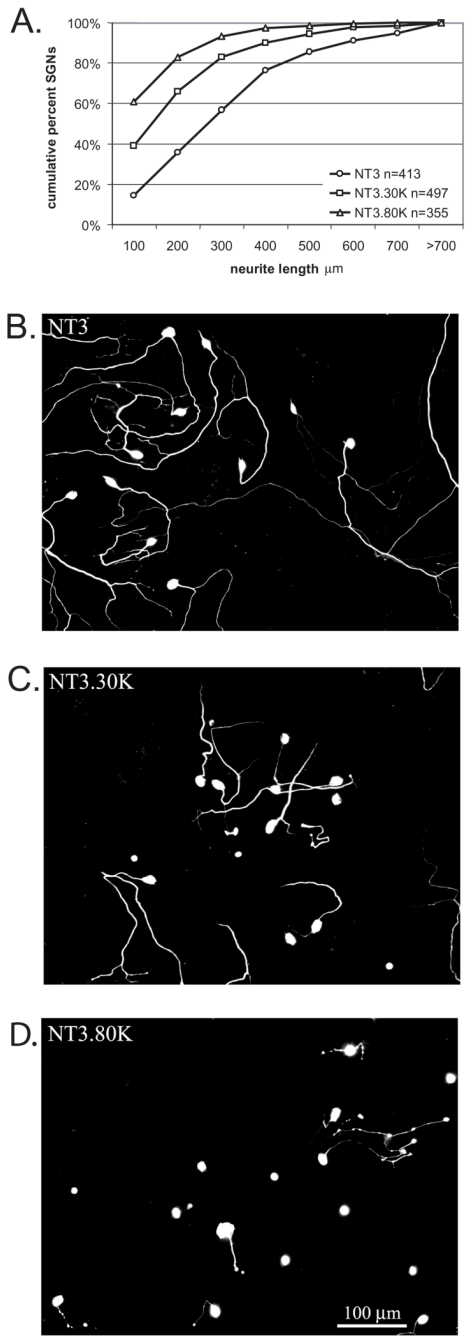

Figure 1.

Membrane depolarization inhibits SGN neurite growth. **A.** SGN cultures were maintained in NT-3 (50 ng/ml), NT-3 with 30 mM $[K^+]_o$ (30K) or NT-3 with 80 mM $[K^+]_o$ (80K) for 48 h. Following fixation, the cultures were immunolabeled with anti-neurofilament 200 (NF-200) antibody followed by a fluorescently conjugated secondary antibody. Neurite length was determined by measuring the longest process extending from each SGN in 5–7 randomly selected fields/well. Results are presented as cumulative percent histograms where conditions with shorter neurites are shifted to the left compared with conditions with longer neurites. Each condition was performed in triplicate and repeated at least three times. n=cumulative number of SGNs scored for all repetitions. Each condition is significantly different ($p<0.05$) from the

others by Kruskal-Wallis ANOVA on Ranks followed by a Dunn's post-hoc comparison. **B–D.** Representative images of spiral ganglion cultures maintained in NT-3 (B), NT-3 with 30K (C), or NT-3 with 80K (D) for 48hr and labeled with anti-NF-200. Scale bar=100 μm.

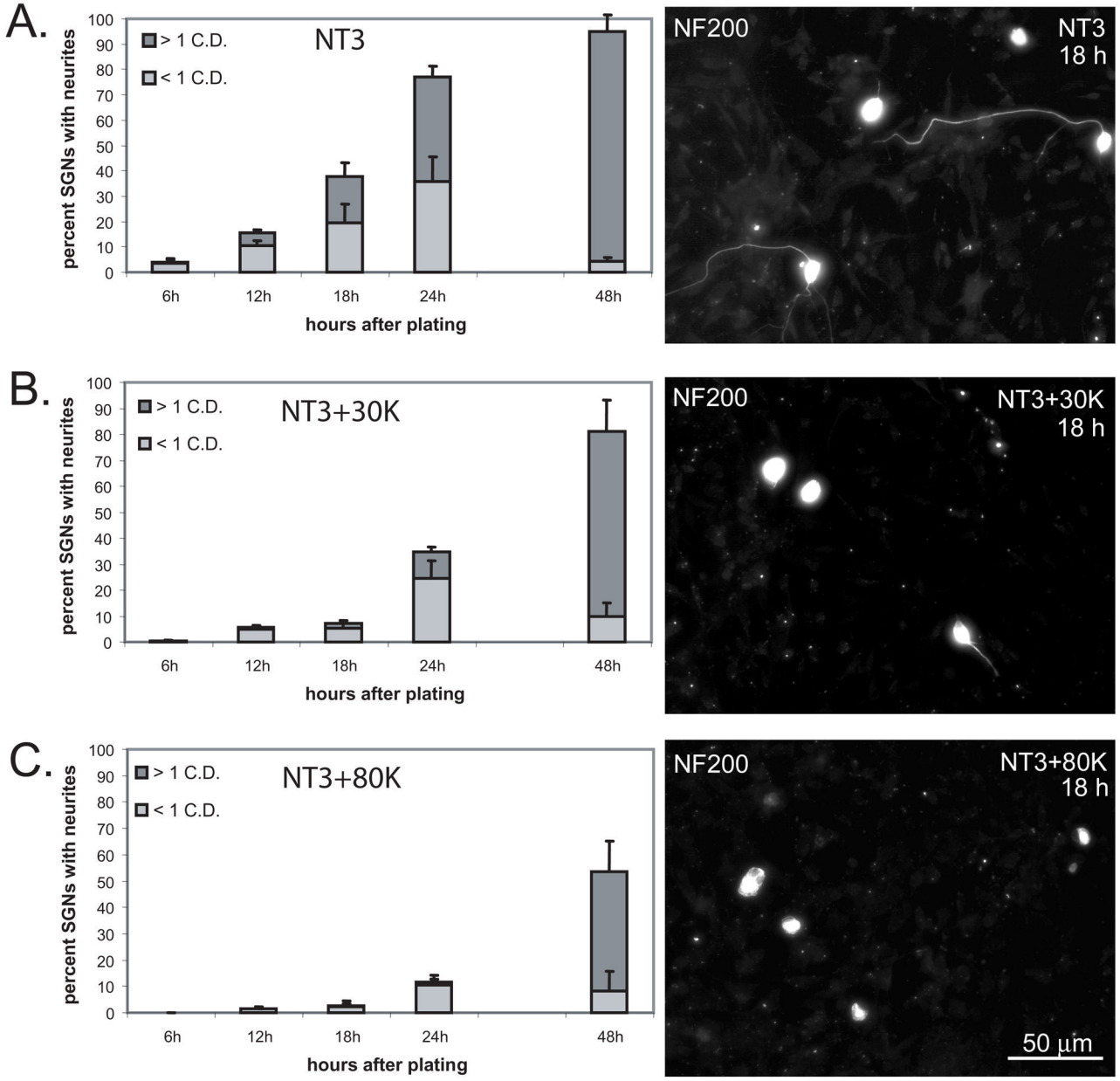

Figure 2.

Membrane depolarization delays SGN neurite initiation. Spiral ganglion cultures were maintained in NT-3 (**A**), NT-3+30K (**B**), or NT-3+80K (**C**) for 6, 12, 18, 24 and 48 hr after plating, fixed, and immunolabeled with anti-NF-200. The percentage of SGNs bearing a neurite < 1 cell diameter (C.D.) or > 1 C.D. was determined for each timepoint. The data presented represent the average of the 3 repetitions and error bars present standard deviation. At 12 hr, a significantly higher percentage of SGNs in NT-3 had a neurite compared with those in NT-3 +30K ($p<0.001$, ANOVA followed by post-hoc Holm-Sidak methodand those in NT-3+80K ($p<0.001$). Similarly, at 12 hr a significantly higher percentage of SGNs in NT-3+30K had a neurite compared with those in NT-3+80K ($p<0.001$). These differences persisted until the 48 hr time point at which point there was no longer a statistically significant difference between the percent of SGNs bearing a neurite in NT-3 compared with those in NT-3+30K ($p=0.057$).

Right panels present representative images of cultures immunostained with anti-NF-200 and maintained in NT-3 (**A**), NT-3+30K (**B**), and NT-3+80K (**C**) for 18 h. Scale bar=50 μm.

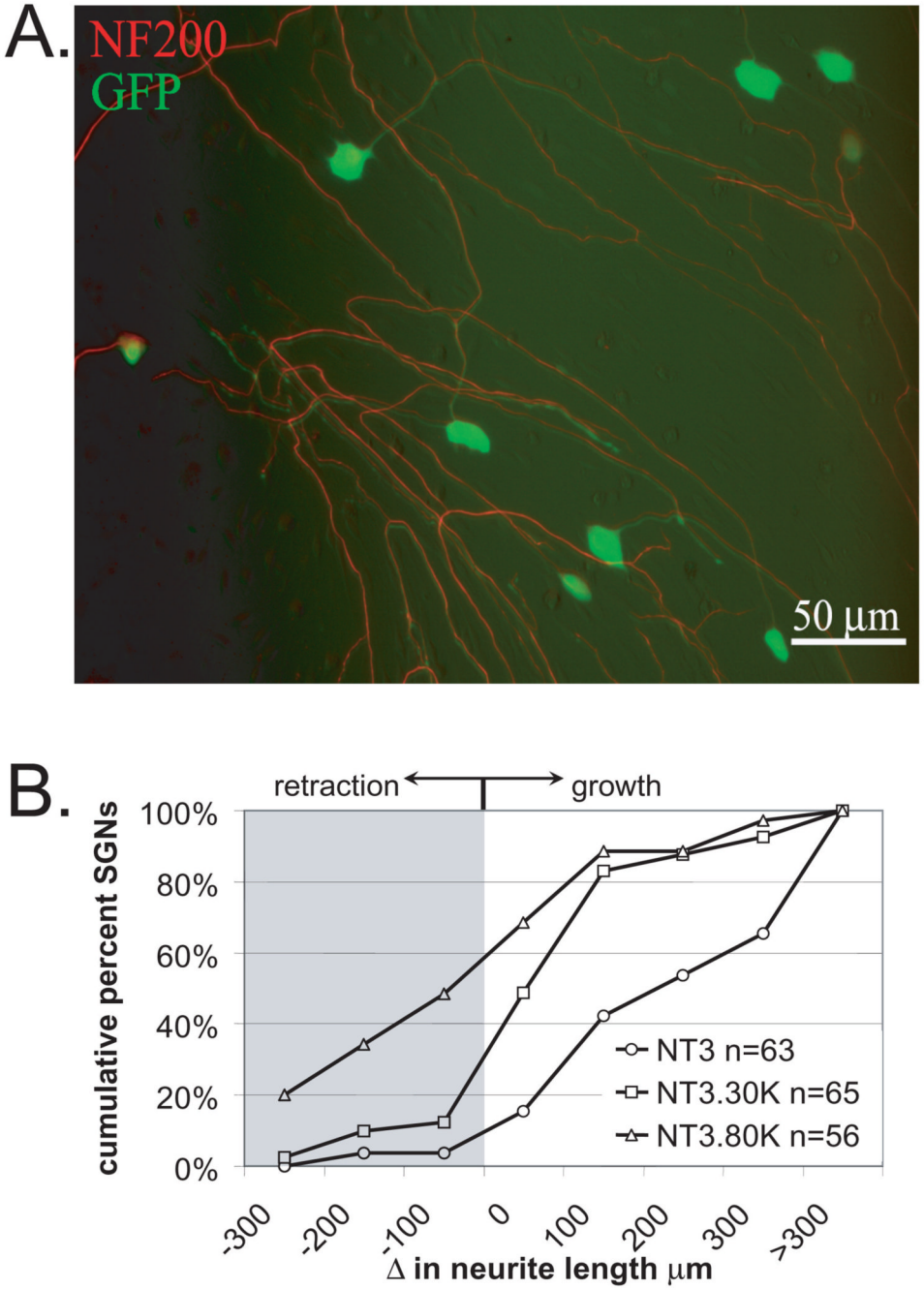

Figure 3.

Membrane depolarization inhibits SGN neurite extension. Spiral ganglion cultures were maintained in NT-3 (50 ng/ml) for 48 hr to allow for neurites to develop. The cultures were then treated with a feline immunodeficiency lentiviral vector encoding green fluorescent protein (FIV-GFP). The GFP fills the entire soma and neurite processes. Initial images of SGNs were captured based on GFP fluorescence. The cultures were then maintained in NT-3, NT-3 +30K, or NT-3+80K for an additional 24 h, fixed, labeled with anti-NF-200 to confirm that imaged processes represented SGN neurites, and reimaged. **A.** Spiral ganglion culture treated with FIV-GFP (green) and labeled with anti-NF-200 followed by an Alexa 568 secondary antibody (red) demonstrating that FIV-GFP transduces a high percentage of SGNs and that the

GFP fills the entire neurite process. In this composite image, the green and red images were offset slightly to better illustrate the overlap of GFP and NF-200 labeling. Scale bar=50 μm. **B.** Change in neurite length over a 24 hr interval for cultures maintained in NT-3, NT-3+30K, or NT-3+80K presented as cumulative percent histograms. Values <0 μm represent neurite retraction while values >0 μm represent neurite growth. Each condition was repeated three times and is significantly different ($p<0.05$) than the others by Kruskal-Wallis ANOVA on Ranks followed by a Dunn's post-hoc comparison. n=cumulative number of SGNs scored for each condition.

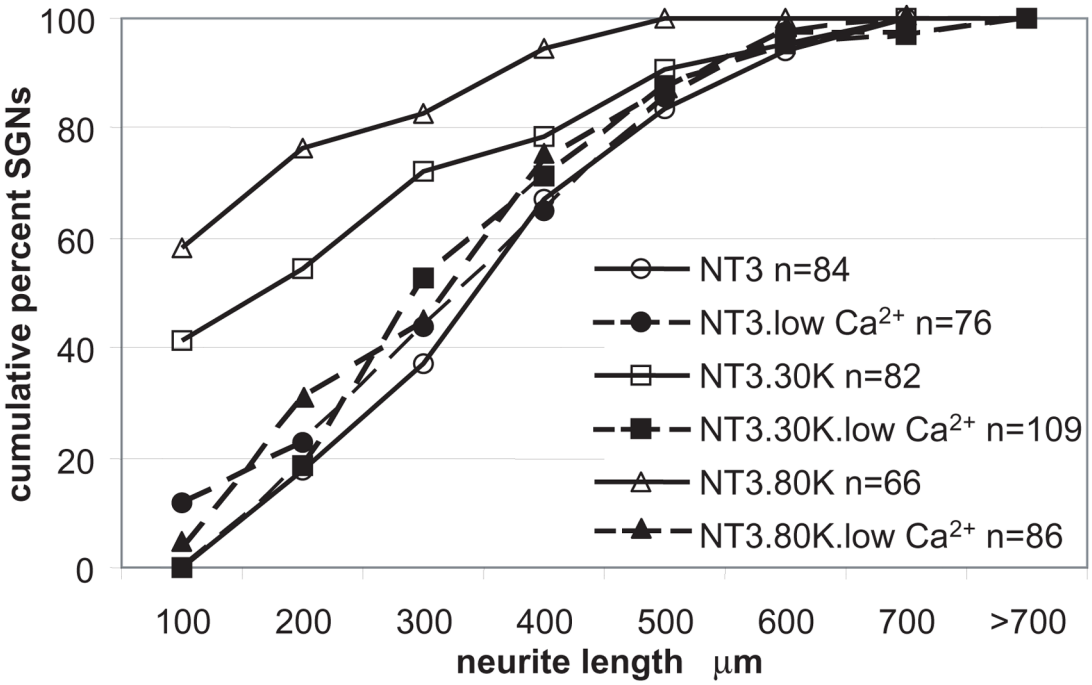

Figure 4.

Removal of Ca^{2+} from the culture medium rescues neurite growth in depolarized SGNs. Spiral ganglion cultures were maintained in NT-3 (50 ng/ml), NT-3 with 30K, or NT-3 with 80K in normal medium or medium lacking Ca^{2+} with EGTA (1 mM) (low Ca^{2+}) for 48 h. Following fixation, neurite length was determined as above. Each condition was repeated three times. n=cumulative number of SGNs scored. NT-3+30K and NT-3+80K are both significantly different ($p<0.05$) from NT-3, NT-3+30K with low Ca^{2+}, and NT-3+30K with low Ca^{2+} by Kruskal-Wallis ANOVA on Ranks followed by a Dunn's post-hoc comparison.

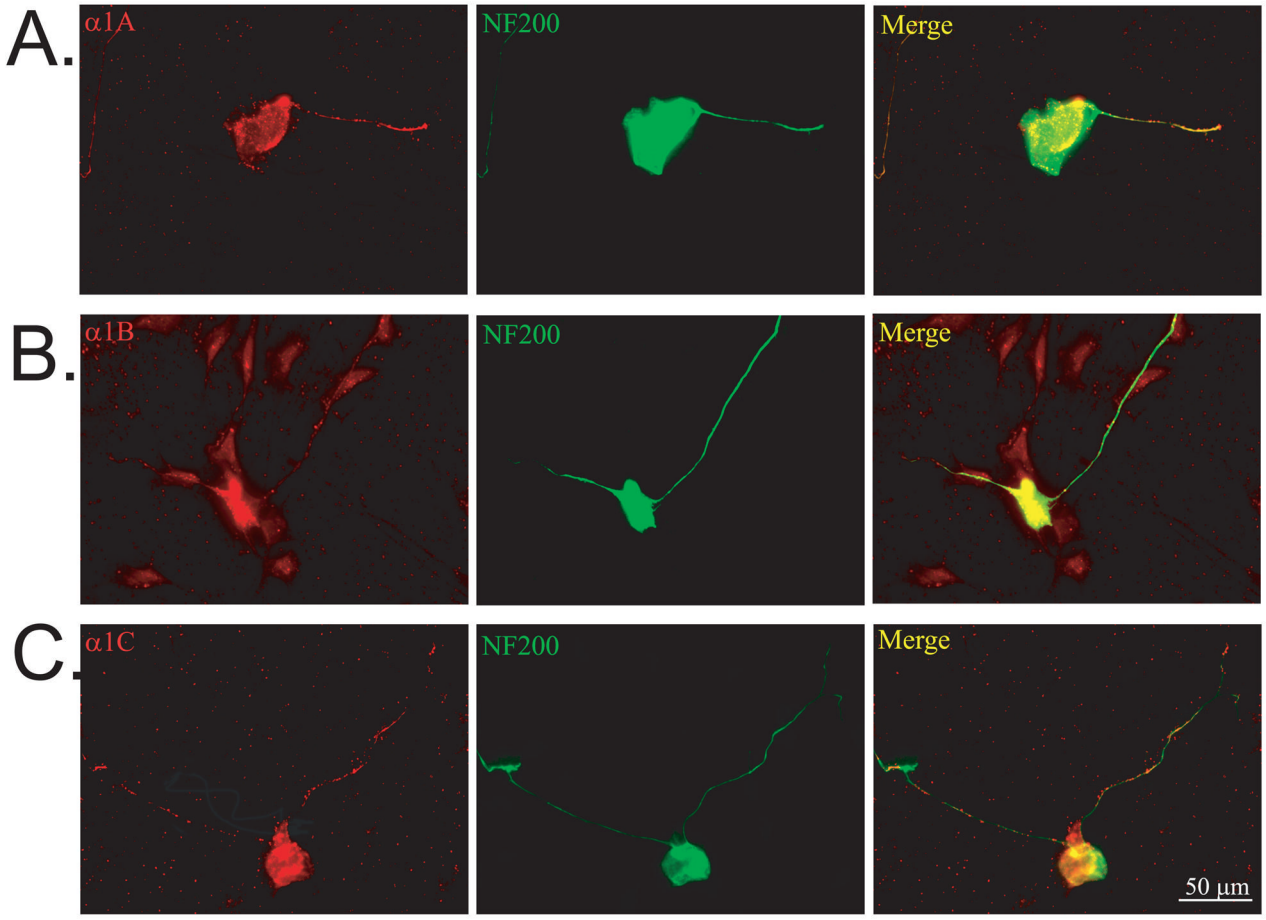

Figure 5.
Spiral ganglion neurons express multiple VGCCs. Spiral ganglion cultures were double immunolabeled with antibodies against anti-α1A (**A**), α1B (**B**), or α1C (**C**) subunits of VGCCs (red, left panels) and anti-NF-200 (green, middle panels). Overlap of VGCCs and NF-200 immunoreactivity appears as yellow and is shown on right panels. Scale bar=50 μm.

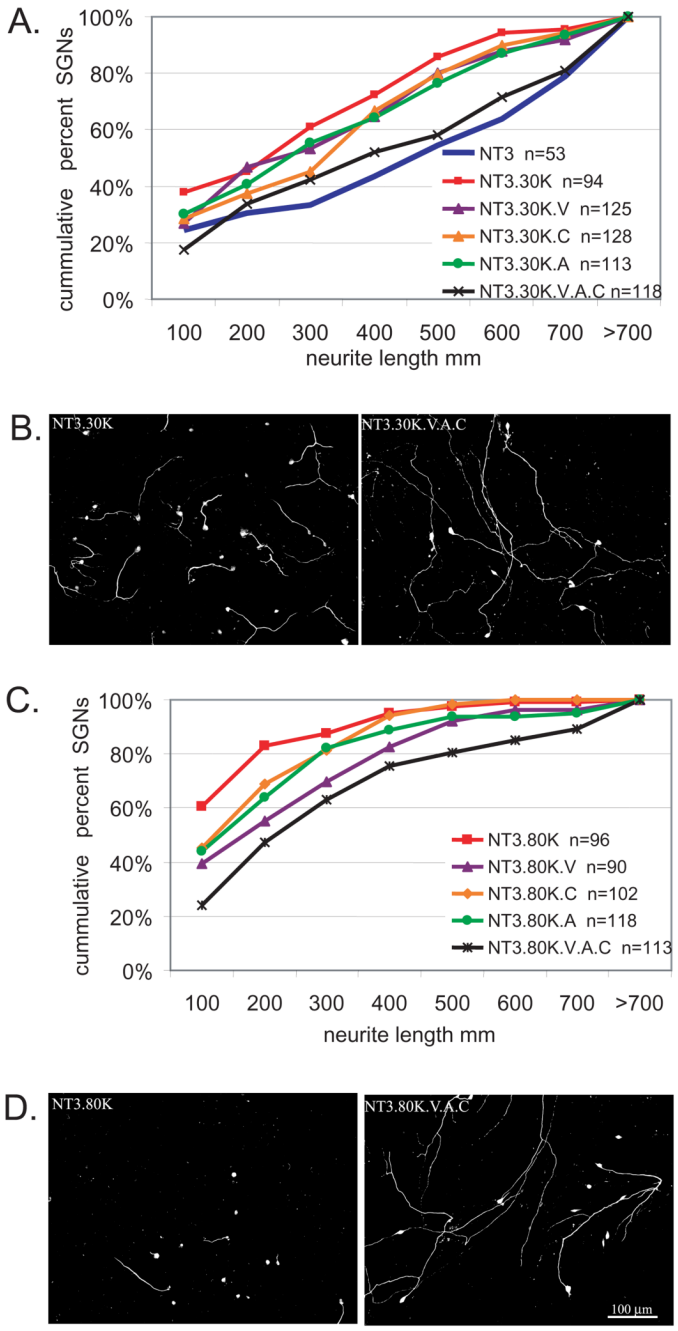

Figure 6.

Multiple VGCCs contribute to the inhibition of neurite growth by depolarization. Spiral ganglion cultures were maintained in the presence or absence of the VGCC antagonists verapamil (V), conotoxin (C), or agatoxin (A) either singly or in combination and neurite length was determined as above. **A**. Cumulative percent histograms of SGN neurite lengths from cultures maintained in NT-3, NT-3+30K, or NT-3+30K with VGCC antagonists. Each condition was repeated three times and is significantly different ($p<0.05$) from NT-3+30K by Kruskal-Wallis ANOVA on Ranks followed by a Dunn's post-hoc comparison. n=cumulative number of SGNs scored for each condition. **B.** Representative images of spiral ganglion cultures maintained in NT-3+30K or NT-3+30K+V+A+C for 48 hr and labeled with anti-

NF-200. **C**. Cumulative histograms of SGN neurite lengths from cultures maintained in NT-3, NT-3+80K, or NT-3+80K with VGCC antagonists. Each condition was repeated three times. NT-3+80K+V and NT-3+80K+V, A, and C are significantly different ($p<0.05$) from NT-3 +80K by Kruskal-Wallis ANOVA on Ranks followed by a Dunn's post-hoc comparison. **D.** Representative images of spiral ganglion cultures maintained in NT-3+80K or NT-3+80K+V, A, and C for 48 hr and labeled with anti-NF-200. Scale bar=100 μm for **B** and **D**.

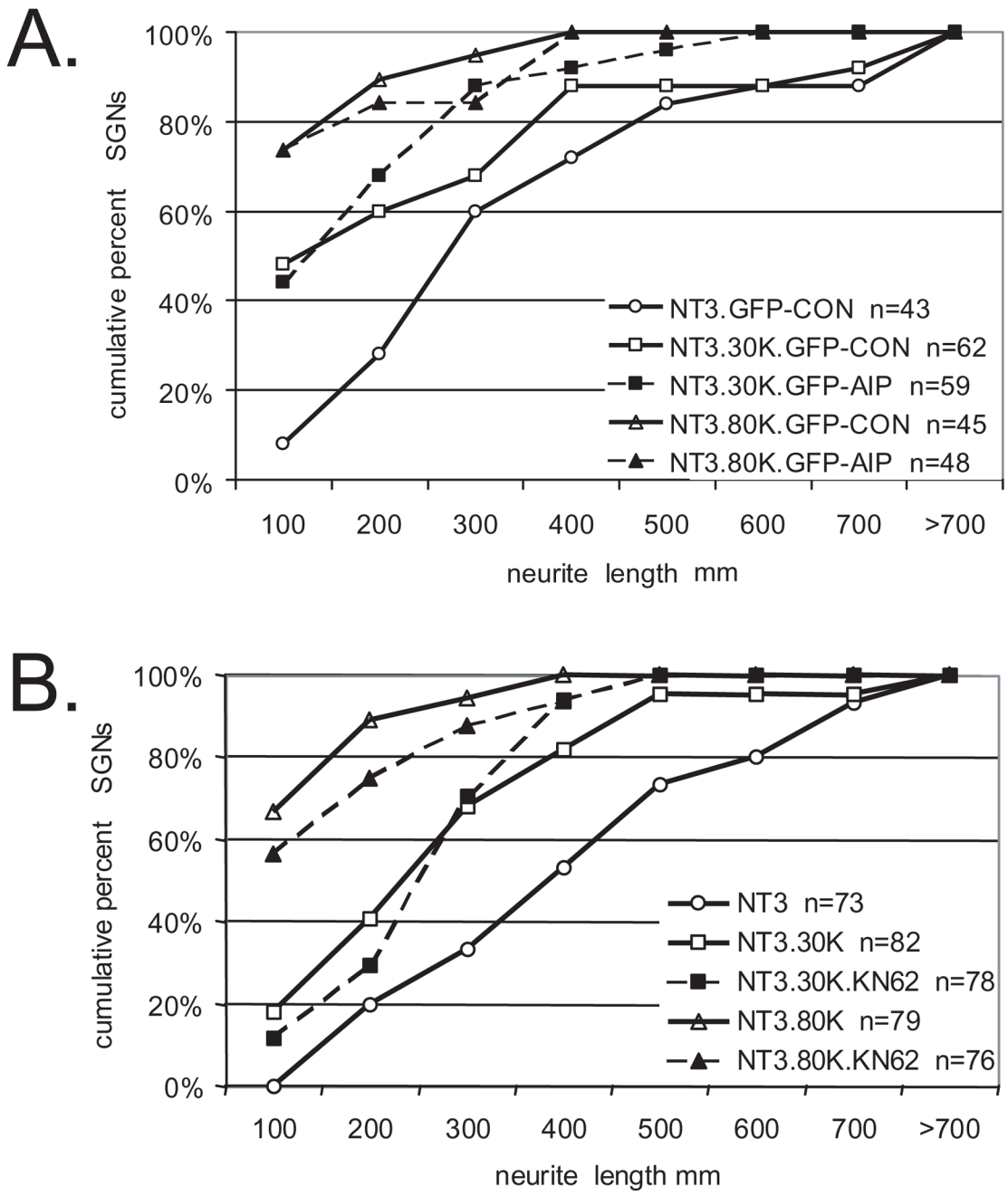

Figure 7.

CaMKII activity is not required for the inhibition of neurite growth by depolarization. **A.** Spiral ganglion cultures were transfected with expression plasmids encoding green fluorescent protein (GFP) -tagged autocamtide-2-related inhibitory peptide (GFP-AIP) or GFP-tagged control (scrambled) peptide (GFP-CON). Cultures were maintained in NT-3, NT-3+30K, or NT-3+80K for 48 hr after transgene expression as indicated. Neurite length for each transfected SGN (GFP+/NF-200+) was scored as before. Each condition was performed in duplicate or triplicate and repeated at least three times. n=cumulative number of SGNs scored for all repetitions. NT-3+30K+GFP-AIP and NT-3+80K+GFP-AIP were not significantly different ($p>0.05$) from NT-3+30K+GFP-CON and NT-3+80K+GFP-CON, respectively, but both were

significantly different than NT-3+GFP-CON ($p<0.05$) by Kruskal-Wallis ANOVA on Ranks followed by a Dunn's post-hoc comparison. **B**. Spiral ganglion cultures were maintained in NT-3, NT-3+30K, or NT-3+80K with or without KN-62 (10 μM) for 48 hr as indicated. Neurite length was determined as above and is presented as cumulative histograms. n=cumulative number of SGNs scored for all repetitions. NT-3+30K+KN-62 and NT-3+80K+KN-62 were not significantly different ($p>0.05$) from NT-3+30K and NT-3+80K by Kruskal-Wallis ANOVA on Ranks followed by a Dunn's post-hoc comparison.

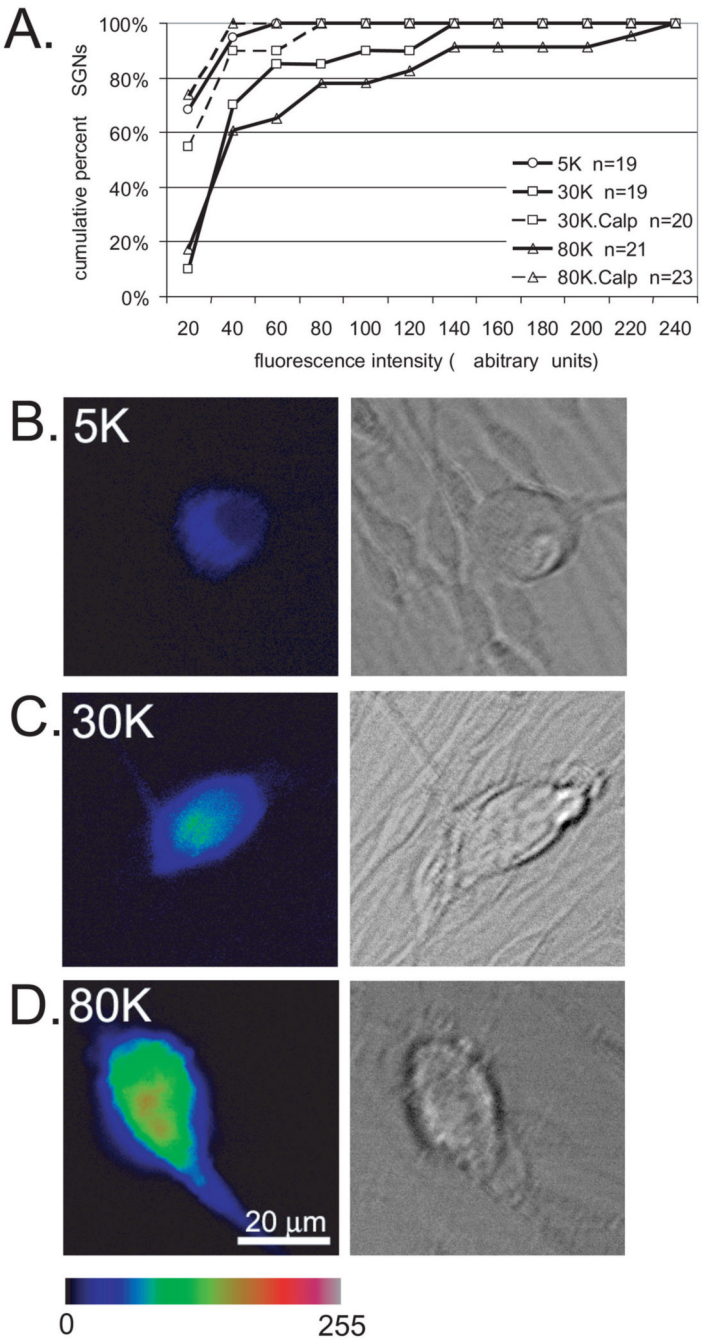

Figure 8.

Calpains are activated by depolarization in SGNs. **A**. Spiral ganglion cultures were loaded with the fluorogenic calpain substrate t-BOC and maintained in control medium (5K) or depolarized with 30K or 80K either in the presence or absence of calpeptin (Calp,10 μM) as indicated. After 15 minutes, images of 15–25 randomly selected SGNs were captured. t-BOC fluorescence intensity was determined by measuring intensity from the neuron cell body after subtracting the background from a similarly sized adjacent region outside the cell body. Fluorescence intensity units are arbitrary. Data are presented as a cumulative histogram and are from one trial. Similar results were obtained in 2 other repetitions. n=number of SGNs scored for this repetition. 30K and 80K are significantly different ($p<0.05$) from 5K and from

30K+Calp and 80K+Calp, respectively by Kruskal-Wallis ANOVA on Ranks followed by a Dunn's post-hoc comparison. **B–D.** Representative images of t-BOC fluorescence (left panels) from SGNs identified based on DIC appearance (right panels) for cultures in 5K (**B**), 30K (**C**), or 80K (**D**). t-BOC fluorescence is presented on an intensity scale of 0–255. Scale bar=20 μm.

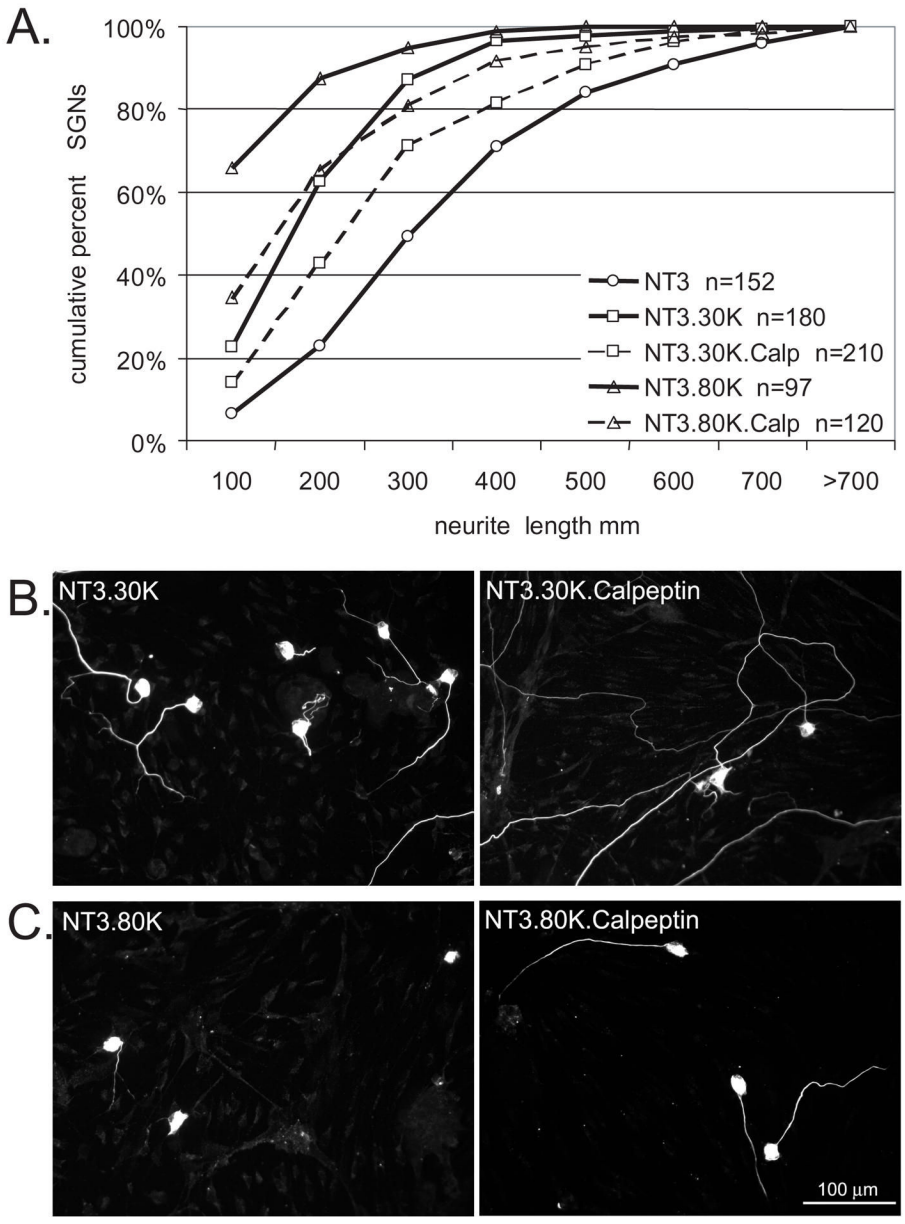

Figure 9.

The calpain inhibitor, calpeptin, rescues SGN neurites from growth inhibition by depolarization. **A**. Cumulative percent histograms of SGN neurite lengths from cultures maintained in NT-3, NT-3+30K, or NT-3+80K with or without calpeptin (Calp,10 μM) as indicated. Each condition was repeated three times. NT-3+30K and NT-3+80K are significantly different ($p<0.05$) from NT-3+30K+Calp and NT-3+80K+Calp, respectively, by Kruskal-Wallis ANOVA on Ranks followed by a Dunn's post-hoc comparison. n=cumulative number of SGNs scored for each condition **B–C.** Representative images of spiral ganglion cultures maintained in NT-3+30K or NT-3+30K+Calp (**B**) and NT-3+80K or NT-3+30K+Calp (**C**) for 48 h and labeled with anti-NF-200. Scale bar=100 μm.